Available online at www.sciencedirect.com
ScienceDirect
International Journal of Pharmaceutics 357 (2008) 260–271
INTERNATIONAL JOURNAL OF PHARMACEUTICS
www.elsevier.com/locate/ijpharm

Pharmaceutical Nanotechnology

A new biocompatible nanoparticle delivery system for the release of fibrinolytic drugs

Anna Maria Piras [a], Federica Chiellini [a,*], Chiara Fiumi [a], Cristina Bartoli [a], Emo Chiellini [a], Bruno Fiorentino [b], Claudio Farina [b]

[a] *Laboratory of Bioactive Polymeric Materials for Biomedical and Environmental Applications (BIOlab)-UdR INSTM, Department of Chemistry & Industrial Chemistry, University of Pisa, Via Vecchia Livornese 1291, 56010 S. Piero a Grado, Pisa, Italy*
[b] *Kedrion S.p.A., Castelvecchio Pascoli, Lucca, Italy*

Received 7 November 2007; received in revised form 14 January 2008; accepted 15 January 2008
Available online 26 January 2008

Abstract

The preparation of novel biocompatible polymeric nanoconstructs suitable to load sensitive bioactive protein agents is reported. Nanoparticles were prepared as based on hybrid polymeric matrices consisting of synthetic bioerodible alternating copolymers of maleic anhydride and *n*-butylvinylether hemiesterified with 2-methoxyethanol and grafted with poly(ethylene glycol) segments and monoclonal antibody single chain fragment specific for fibrin clot.

The prepared nanoparticles were loaded with proteolytic enzymes (trypsin and urokinase), encapsulating up to 2500 UI of urokinase/mg of dried nanoparticles. The release of the enzyme from nanoparticles resulted time controlled and it was assessed that in case of administration of urokinase-loaded nanoparticles, the enzyme would preserve its thrombolytic properties more efficiently in respect to free drug administration. Moreover, the nanoparticles showed a good *in vitro* biocompatibility, suitable for biomedical applications. The stability (shelf life) of the prepared nanostructured dosage forms was evaluated. The drug-loaded nanoparticles resulted stable under stressed conditions (35 °C for 13 weeks) in a lyophilized form and preserved their morphological and functional characteristics when stored in suspension for 18 months at 4 °C.

Keywords: Nanoparticles; Bioactivated polymers; Protein delivery; Enzyme

1. Introduction

Drug-releasing nanoparticles piloted by monoclonal antibodies or specific ligands belong to the third generation of drug delivery systems (Kubik et al., 2005) and represent a powerful tool for the administration of thrombolytic agents, typically associated with the systemic activation of the fibrinolytic system and the incoming of serious side effects (Bell, 2002).

Urokinase is a physiological protein acting as thrombolytic agent, that is often used for peripheral intravascular thrombus, pulmonary embolism, myocardial stroke and as adjunctive therapy after angioplasty of an occluded coronary artery (Katzung, 2000; Barlow and Lazer, 1972; Bernik et al., 1974). Urokinase half-life in plasma is approximately 15 min and it needs to be administered repeatedly in order to keep its concentration inside the therapeutic window. Moreover, the administration of current thrombolytic agents induces the systemic activation of the fibrinolytic system, alters the aggregating healthy interactions of blood components thus causing the incoming of serious bleedings (Craig and Stitzel, 1994). The employment of nanoparticles for the targeted delivery of urokinase may overcome the formation of the mentioned side effects by selectively activating the fibrinolytic system on the pathologic site (bioavailability optimization) as well as by enhancing the half-life of

Abbreviations: GIG-βCD, 1-*O*-glycidyl-2,2-*O*-isopropyldenglycerol-β-cyclodextrin; UK, human urokinase; VAG, best HAS-loaded nanoparticle formulation; VAM41, 2-methoxyethanol hemiester of poly(maleic anhydride-*alt*-butyl vinyl ether); VAM41–Fab, VAM41 grafted with anti-fibrin monoclonal antibody Fab fragment; VAM41–PEG, 2-methoxyethanol hemiester of poly(maleic anhydride-*alt*-butyl vinyl ether) 5% grafted with poly(ethylene glycol); VAM41–PEG–Fab, VAM41–PEG grafted with anti-fibrin monoclonal antibody Fab fragment; VAM41-Sx, VAM41 polymer series with molecular weight range: 300,000–30,000 g mol^{-1}.

* Corresponding author. Tel.: +39 050 2210305; fax: +39 050 2210332.
E-mail address: federica@ns.dcci.unipi.it (F. Chiellini).

0378-5173/$ – see front matter © 2007 Elsevier B.V. All rights reserved.
doi:10.1016/j.ijpharm.2008.01.035

the enzyme in circulation and by reducing the administration dose.

Aim of the present work was the development of a model study for the design and preparation of biocompatible/bioerodibile nanoparticle drug delivery systems for the targeted delivery of protein drugs with proteolytic activity. A putative application was first individuated, taking into account the problematic of current therapeutic protocols based on proteic drug. Therefore, the formulation of Urokinase-loaded nanoparticles to be targeted towards fibrin cloth was selected. At first, experiments were carried out by using easy available proteins as models for the setup of the formulation parameters. Albumin was employed at the beginning of the study, followed by the coformulation with trypsin as a model biomolecule endowed with proteolytic activity and then with the therapeutically applied thrombolytic agent human urokinase. Both trypsin and urokinase belong to the serine protease family and display high homology in terms of sequence alignment, especially in the catalytic site (Lkjaersig et al., 1958; Bergstrom et al., 2003). The preparation of nanoparticles was accomplished by the *co-precipitation* technique in which the polymeric material gives rise to microphase separation because of its low-water solubility and concurrent interaction with protein molecules leads to nanoparticle formation. This original straightforward procedure, developed by the research group involved in the present study (Cowdall et al., 1999a, 1999b), appears advantageous for the loading of protein drugs into a polymer matrix. Indeed, this methodology does not entail the use of chlorinated solvents and it does not require vigorous shear mixing, thus preventing the appreciable denaturation of the entrapped protein molecule typical of other techniques (Park et al., 1995; Zambaux et al., 1999; Pawar et al., 2004).

The study was carried out on 2-methoxyethanol hemiesters of poly(maleic anhydride-*alt*-butyl vinyl ether) having different molecular weights and previously characterized as bioerodible, biocompatible polymeric material for biomedical application (Chiellini et al., 1992, in press). 1-*O*-glycidyl-2,3-*O*-isopropylidenglycerol-β-cyclodextrin, was applied as formulation stabilizer (Breschi et al., 1996; Chiellini et al., 1991). Stealth and site-specific targeting features were displayed on nanoparticles surface by using pegylated polymer matrices and anti-fibrin monoclonal antibody Fab fragments grafted on the bioerodible polymers.

2. Experimental

2.1. Materials

All reagents were purchased from Carlo Erba (Rodano, MI, Italy), if not otherwise stated. Ethanol, porcine trypsin and sodium azide were purchased from Sigma–Aldrich (St. Louis, MO, USA); trizma buffer from BioChemika (Sigma–Aldrich, St. Louis, MO, USA); human serum albumin (HSA) 25% in solution, and human urokinase (UK) (Afakinasi, 100,000 UI, Alfa Wassermann S.p.A., Bologna, Italy) were kindly supplied by Kedrion S.p.A. (Castelvecchio Pascoli, LU, Italy) 1-*O*-glycidyl-2,3-*O*-isopropylidenglycerol-β-cyclodextrin (GIG-βCD), 2-methoxyethanol hemiester of poly(maleic anhydride-*alt*-butyl vinyl ether) (VAM41 series), VAM41 5% grafted with poly(ethylene glycol) (PEG2000) (Mw 2000 g mol^{-1}, Aldrich) (VAM41–PEG), human anti-fibrin Fab grafted VAM41 (VAM41–Fab) and Human anti-fibrin Fab grafted VAM41–PEG (VAM41–PEG–Fab) were prepared either in our facilities (Chiellini et al., in press) or kindly provided by Polymer Laboratories Ltd., Church Stretton, UK (Table 1).

Table 1
Bioerodible 2-methoxyethanol samples of maleic anhydride/butylvinylether alternating copolymer employed in the preparation of nanoparticles

Polymer	Mw (g mol^{-1})
VAM41-S0	324,000
VAM41-S1	180,000
VAM41-S2	133,000
VAM41-S3	126,000
VAM41-S4	103,000
VAM41-S5	64,000
VAM41-S6	30,000
VAM41-S7	28,000
VAM41[a]	130,000
VAM41–Fab	29,000[b]
VAM41–PEG	38,000[b]
VAM41–PEG–Fab	40,000[b]

[a] Pilot-scale batch, provided by Polymer Laboratories Ltd.
[b] Theoretical molecular weight.

Balb/3T3 Clone A31 (ATCC CCL163) mouse embryo fibroblast cell line was purchased from ATCC (American Tissue Culture Collection, LGC Promochem srl Sesto San Giovanni, MI, Italy) and propagated following the instructions provided by the supplier. Penicillin, Streptomycin, Calf Serum (CS), Glutamine, Phosphate Buffer Saline without Ca^{2+} and Mg^{2+} (PBS) 0.01 M pH 7.4, and trypsin: EDTA containing 0.25% trypsin were purchased from Gibco (Invitrogen Carlsbad, CA, USA). Complete Dulbecco's Modified Eagles Medium (complete DMEM) solution was prepared by adding penicillin (100 U/ml), streptomycin (100 μg/ml), glutamine (4 mM) and 10% fetal bovine serum to DMEM (Gibco, Invitrogen Carlsbad, CA, USA). Cell proliferation reagent (WST-1) was obtained from Roche Molecular Biochemicals (Indianapolis, IN, USA).

2.2. Preparation of HSA-loaded nanoparticles

Nanoparticle suspensions were prepared by applying the co-precipitation technique to VAM41-Sx polymers having different molecular weights (Table 1) and to the polymers functionalized with PEG moieties and anti-fibrin monoclonal antibody Fab fragments (VAM41–PEG, VAM41–Fab, VAM41–PEG–Fab). In general, the polymers were dissolved in 4:1 ethanol/water solutions and added drop-wise (22G needle) to a solution of deionised water, containing GIG-βCD and HSA, kept under magnetic stirring. The dropping rate was adjusted to 30 drops/min and the process took place at room temperature. For all pegylated polymers, the pH of polymer solution was adjusted to 4.5 before dropping. All nanoparticle formulations were performed in triplicates and preparation details are reported in Table 2.

Table 2
Ingredients utilized in the nanoparticle formulations

Run (mg)	Polymer[a] (mg)	Solvent[b] (ml)	GIG-βCD (mg)	HSA (mg)	Enzyme (mg)	Water (ml)
VAGO	100	2.0	250.0	20	–	5.0
VAGV	35	3.5	87.5	14	–	3.5
VAG[c]	50	2.0	125.0	10	–	5.0
VAGA	50	2.0	125.0	20	–	5.0
VAGG	50	2.0	250.0	10	–	5.0
VAGAG	50	2.0	250.0	20	–	5.0
10TVAG[d]	50	2.0	125	9.0	1.0	5.0
10UVAG[e]	50	2.0	125	9.0	1.0	5.0

[a] VAM41-S0.
[b] 4:1 ethanol/water mixture.
[c] Prepared with all VAM41-Sx polymers, pegylated and Fab-grafted polymers.
[d] Trypsin-loaded nanoparticles, the formulation was applied to all VAM41-Sx polymers, pegylated and Fab-grafted polymers.
[e] Urokinase-loaded nanoparticles, the formulation was applied to low molecular weight polymers VAM41-S6 and VAM41-S7, pegylated and Fab-grafted polymers.

2.3. Preparation of enzyme-loaded nanoparticles

2.3.1. Preparation of trypsin-loaded nanoparticles

The preparation of trypsin-loaded nanoparticles was carried out as described above. Trypsin powder was dissolved in PBS to final 1% (w/v) concentration and added to the water solution of GIG-βCD and HSA, as reported in Table 2.

2.3.2. Preparation of urokinase-loaded nanoparticles

Urokinase-loaded nanoparticles were prepared by replacing porcine trypsin with human urokinase (UK) in 10TVAG formulation and by using low molecular weight VAM41-Sx and the biofunctionalized VAM41–PEG, VAM41–PEG–Fab polymers. 70000 UI (corresponding to 1 mg of enzyme) were utilized for the preparation of standard volumes (7 ml) of nanoparticles suspensions. UK was previously dissolved in PBS to a final concentration of 500 UI/μl and then added to the GIG-βCD, HSA solution (Table 2).

All nanoparticle formulations were performed in triplicates.

2.4. Nanoparticles purification

Nanoparticle suspensions were purified by centrifugation in ALC® (Cologno Monzese, MI, Italy) PK121R centrifuge at $8000 \times g$ for 30 min, at 4 °C and the pellets were suspended in appropriate medium depending on the type of analysis.

2.5. Nanoparticles characterization

2.5.1. Granulometry in suspension

Dimensional analyses were carried out by Coulter LS230 Laser Diffraction Particle Size Analyzer (Beckman Coulter Fullerton, CA, USA), equipped with *small volume module plus.* Diameter distribution was processed using Fraunhofer optical model. Three runs were performed on each sample.

2.5.2. Morphological analysis

Nanoparticle morphology was investigated by means of scanning electron microscopy (SEM, JEOL LSM5600LV, Tokyo, Japan). The samples were prepared from the purified and lyophilized nanoparticles (5Pascal Lio 5P, Trezzano sul Naviglio MI, Italy).

2.5.3. Zeta potential analysis

Zeta potential analyses were carried out by using a Coulter Beckman Delsa 440SX (Beckman Coulter Fullerton, CA, USA) at 25 °C with a 0.4 °C tolerance between upper and lower sensors. Nanoparticle suspensions were purified, re-dispersed in 0.9% NaCl solution, pH 5–5.2, and diluted to a final concentration of 0.1 mg/ml. Zeta potential values were calculated as the mean value of 10 replicates for each nanoparticle formulation.

2.5.4. Evaluation of human serum albumin incorporation

The extent of HSA incorporation in nanoparticles was evaluated by the colorimetric assay Pierce (Rockford, IL, USA) Micro BCA™ Protein Assay and plate reading was performed on a Bio-Rad Benchmark Microplate Reader (Bio-Rad, Hercules, CA, USA). Nanoparticles were separated from the material not converted into nanoparticles by prolonged high-speed centrifugation ($15{,}900 \times g$ for 120 min at 4 °C). Protein incorporation was calculated as the difference between total HSA employed in the preparation of the nanoparticles and the unconverted protein measured in the supernatants. Standard curve was obtained by plotting the average blank-corrected absorbance of each standard *vs.* its HSA concentration (5–80 μg/ml; $R^2 = 0.9982$). Four different dilutions of each nanoparticles supernatant were assayed in triplicate.

2.5.5. Evaluation of trypsin encapsulation

Trypsin encapsulation in nanoparticles was evaluated by means of size exclusion chromatography (SEC). The chromatographic system consisted of a quaternary gradient unit JASCO LG-1580-04, JASCO PU-1580 intelligent HPLC pump, JASCO UV-1575, JASCO 830 RI (Jasco, Oklahoma City, OK, USA), equipped with a styrene–divinyl benzene guard column (500 Å, 5 μm) and linear 6–13 μm (300 mm × 7.5 mm) ultrahydrogel columns (Waters, Milford, MA, USA). The mobile phase consisted of PBS, 0.2 μm filtered, and flow rate was maintained at 0.8 ml/min. UV–vis detection occurred at 280 nm and all analyses were performed at 40 °C. Trypsin standard curve (10–250 μg/ml; $R^2 = 0.9998$) was calculated

from the UV-detected chromatograms. Nanoparticle samples were prepared from purified trypsin-loaded nanoparticle pellets and supernatants; HSA-loaded nanoparticles were used as blank. Three replicates were prepared for each specimen. All samples were left under magnetic stirring at 4 °C for 24 h to allow complete nanoparticles dissolution in PBS, before analysis.

2.5.6. Evaluation of the activity of encapsulated trypsin

The trypsin activity was evaluated by a colorimetric assay using *N*-α-benzoyl-D,L-arginine-4-nitroanilide (BApNA) as synthetic substrate. Experiments were carried out on purified nanoparticles pellets dissolved in PBS, and relative supernatants. The samples (100 μl) were incubated 60 s with 100 μl of 0.50 mM BApNA solution in PBS at room temperature and absorbance at 405 nm was measured by a microplate reader. HSA-loaded nanoparticles were used as blank. The active trypsin concentration was determined on standard calibration curves (10–100 μg/ml; $R^2 = 0.9992$).

Trypsin proteolytic activity toward a natural macromolecular substrate such as HSA was investigated by means of SEC and the experimental parameters were set as described above. Experiments were carried out on purified trypsin-loaded nanoparticle pellets and HSA-loaded nanoparticles were used as negative control. The pellets were dissolved in PBS at 4 °C. HSA substrate was then added and SEC runs were performed after incubation at room temperature for 24 and 48 h.

2.5.7. Evaluation of the activity of the encapsulated urokinase

Urokinase activity was evaluated by a colorimetric assay using S-2444 (Chromogenix, Milano, Italy) reagent as synthetic substrate. Experiments were carried out on UK-loaded nanoparticles and HAS-loaded nanoparticles were used as blank. 100 μl of nanoparticles samples were incubated at room temperature with 100 μl of 0.6 mM S-2444 solution in PBS. ΔABS/min at 405 nm was calculated over 5 min of reaction. The active urokinase concentration was determined on standard calibration curve (250–1500 UI/ml; $R^2 = 0.9982$).

2.5.8. In vitro drug release studies

Release kinetics studies were performed on UK-loaded nanoparticles and naked nanoparticles by using Spectra/Por (Spectrum Laboratories, Rancho Dominguez, CA, USA) regenerated cellulose membranes (MWCO 60000 Da). 40 ml of each nanoparticle sample were purified and re-dispersed in 2.0 ml of PBS 0.05 M pH 7.4. 80,000 UI/ml urokinase solution was used as control. Dialysis was performed against 30 ml of 0.2% EDTA solution in PBS 0.05 M pH 7.4, at 37 °C. 2 ml of the external medium were withdrawn and replaced with fresh buffer at fixed times. Protein release was quantified on a HSA standard curve by means BCA assay (10–100 μg/ml; $R^2 = 0.9943$). The maintenance of UK activity was investigated by means of the chromogenic assay S-2444 by using UK standard curve (100–1000 UI/ml; $R^2 = 0.9825$).

2.6. Assessment of nanoparticles stability

2.6.1. Stability of lyophilized nanoparticles

HSA-loaded nanoparticles prepared with VAM41 were purified, 0.2 μm filtered under laminar flow cabinet and freeze-dried under sterile conditions (freezing at −20 °C; 5Pascal Lio 5P). Nanoparticles underwent stressed (35 ± 2 °C, for 13 weeks, 2 samples analysed weekly) and accelerated (25 ± 2 °C, for 6 months, 2 samples analysed monthly) stability studies upon storage in W85RF oven (KW s.r.l., Monteriggioni SI, Italy); the stability was assessed by monitoring nanoparticle morphology.

10UVAG-S7 (UK-loaded) nanoparticles underwent stressed stability studies. Nanoparticles pellets were re-dispersed in sterile 0.2% EDTA–7% mannitol solution, freeze-dried and sealed under vacuum. A 500 UI/ml urokinase solution in 0.2%–EDTA 7% mannitol was sterilised and lyophilized as reference for the stability study. Nanoparticles stability was investigated by measuring both enzyme activity and nanoparticles diameter distribution maintenance after re-dispersing the lyophilized powder in water.

2.6.2. Stability of nanoparticle suspensions

HSA-loaded nanoparticles prepared with VAM41 were sterilised by 0.2 μm filtration under laminar flow cabinet and kept either in the dark at 4 °C or at room temperature (21 ± 3 °C). Granulometry in suspension was performed after 3, 6, 9, and 15 months.

Purified UK-loaded nanoparticles (10UVAG-S7) were sterilised by 0.45 μm filtration under laminar flow cabinet and stored for 16 months in the dark, at 4 °C. Nanoparticles stability was assessed by granulometry in suspension and activity assay.

2.7. In vitro assessment of cytotoxicity

Cytotoxicity of nanoparticles was assessed by measuring the viability of balb 3T3/Clone A31 fibroblasts grown in DMEM medium containing the prepared polymeric nanostructured systems. Quantitative analyses of cell viability and proliferation were performed by WST-1 assay.

Bioerodible nanoparticles were purified, freeze-dried, weighed, and re-dispersed in complete DMEM to a final concentration of 5 mg/ml. A subconfluent monolayer of Balb3T3/Clone A31 fibroblasts was trypsinized using a 0.25% trypsin 1 mM EDTA solution. Cells were centrifuged at 1000 rpm for 5 min, re-dispersed in complete DMEM medium and counted. 3×10^3 cells per 100 μl of medium were placed in each well of flat-bottom 96-microwell plates. Plates were incubated at 37 °C, 5% CO_2 for 24 h until 60–70% cell confluence was reached. The medium from each well was then removed and replaced with a fresh medium containing nanoparticles. Control cells were incubated with fresh growth medium, whereas only growth medium was used as blank.

After 24 h incubation, cells were incubated with WST-1 Cell Proliferation Reagent diluted 1:10 for 4 h at 37 °C, 5% CO_2. Plates were then analyzed with a Bio-Rad Benchmark Microplate Reader (Bio-Rad, Hercules, CA, USA). The number of viable cells was evaluated from the sample absorbance at

450 nm diminished by the blank absorbance at the same wavelength and by using 620 nm as reference wavelength.

Optical microscopy observations of cells were performed by using a Nikon Eclipse TE 2000 inverted microscope equipped with epifluorescence lamp and Nikon D Eclipse C1 confocal system (Nikon, Tokyo, Japan).

All experiments were performed in triplicates

3. Results and discussion

3.1. HSA-loaded nanoparticles

The setup of conditions for nanoparticle formulations represents the first stage for the preparation of the nanostructured drug delivery system under investigation.

Preliminary tests were performed in order to assess the effectiveness of the co-precipitation technique in the preparation of nanoparticles by using the high molecular weight VAM41-S0 polymer, HSA and the stabilizer GIG-βCD. In VAM41-S0 particles formulation, it was observed that polymer concentration and volume ratio between organic and aqueous solutions mostly affect the homogeneity of the suspensions and the diameter distribution of the particles. Either high polymer concentration (VAGO) and 1:1 volume ratio (organic:aqueous solutions) (VAGV) determine a polymodal diameter distributions and the formation of macroscopic aggregates. Differently, variations of either HSA or stabilizer concentrations did not significantly affect particle diameter distribution. The encapsulation efficiency of nanoparticles toward HSA was considered as a primary parameter for the selection of the best naked nanoparticle formulations (Fig. 1, Table 3). Beside polymodal diameter distribution, formulation VAGV gave the lowest HSA incorporation. The other formulations that differed in HSA and GIG-βCD concentrations led to high incorporation percentages, ranging between 67% and 85%. It is worth mentioning that protein incorporation increased with the concentration of the stabilizer employed in the formulation.

Based on the above reported results, VAG formulation was selected for the subsequent enzyme loading and biofunctionalization investigations. VAG formulation led to a homogeneous

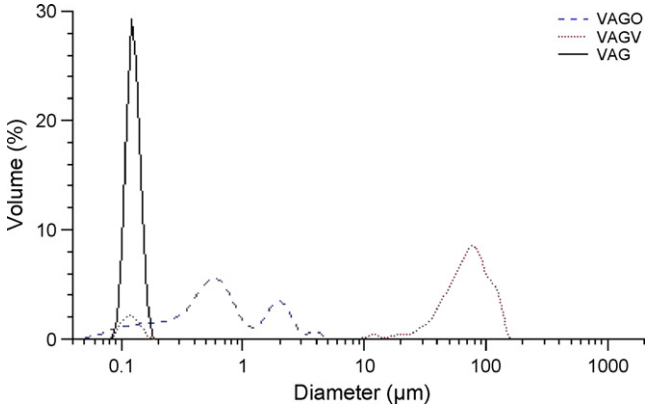

Fig. 1. Diameter size distribution of nanoparticles prepared under different formulation conditions.

Table 3
Determination of content of human serum albumin (HSA) loading into nanoparticles

Run (nm ± S.D.)	Diameter[a] (% ± S.D.)	HSA Inc.[b]
VAGO	867 ± 794	–
VAGV	61.1 ± 38.4[c]	40 ± 14
VAG	132 ± 16	67 ± 6
VAGA	131 ± 16	69 ± 8
VAGG	132 ± 16	77 ± 6
VAGAG	147 ± 20	85 ± 4

[a] Diameter distribution by vol.%.
[b] Incorporation of HSA with respect to the total amount involved in the preparation of the nanoparticles.
[c] μm ± S.D.

suspension containing nanosized particles with monomodal diameter distribution and despite the low amount of materials involved in the preparation of the nanoparticles, protein incorporation percentage is nearly 70%, suggesting that there is an optimized employment of the materials. VAG formulation was successfully applied to the entire series of VAM41-Sx polymers, having different molecular weights. All the prepared nanoparticles displayed an average diameter in the range of 125–130 nm with a narrow standard deviation (15–20 nm), highly reproducible results. It was observed that the application of the co-precipitation technique to VAM41-Sx polymers with molecular weight ranging from 324,000 to 28,000 g mol^{-1}, being the latest a molecular weight value below the renal excretion threshold, had no major influence on particle size, diameter distribution and morphology (Fig. 2A). Hence, it is feasible that once nanoparticles have complete their drug-releasing function in the body, VAM41-S6 and -S7 polymers would be easily eliminated (Hoste et al., 2000).

Long-circulating nanoparticles and biofunctionalized nanoparticles carrying targeting moieties on their surface were prepared by co-precipitation, following VAG formulation conditions. Surface modification was achieved by using pegylated and biofuncionalised polymers grafted with Fab–SH fragments specific for fibrin γ-epitope, during the preparation process. The use of pegylated polymers required an adjustment of the pH of polymer solution, before dropping. The acidic pH was necessary to induce the co-precipitation, by reducing the solubility of the polymer in aqueous solution and shielding the effect of PEG chains that would conversely enhance polymer water solubility and prevent nanoparticle formation.

Nano-sized particles with monomodal diameter distribution and average diameter of 130 ± 16 nm were obtained. Zeta potential analyses were performed under physiological solution in order to emphasizes the difference in nanoparticles surface charge and highlights the steric hindrance due to the exposure of PEG and Fab moieties. Moreover, the detection of changes related to the presence of Fab moieties exposed on nanoparticle surface provided evidence to the stability of the covalent linkage between Fab–SH and the polymer matrix during nanoparticle preparation process. As shown in Table 4, Fab–SH fragments and PEG chains had an opposite effect on nanoparticles surface charge when the zeta potential of VAG-S7 (naked nanoparticles)

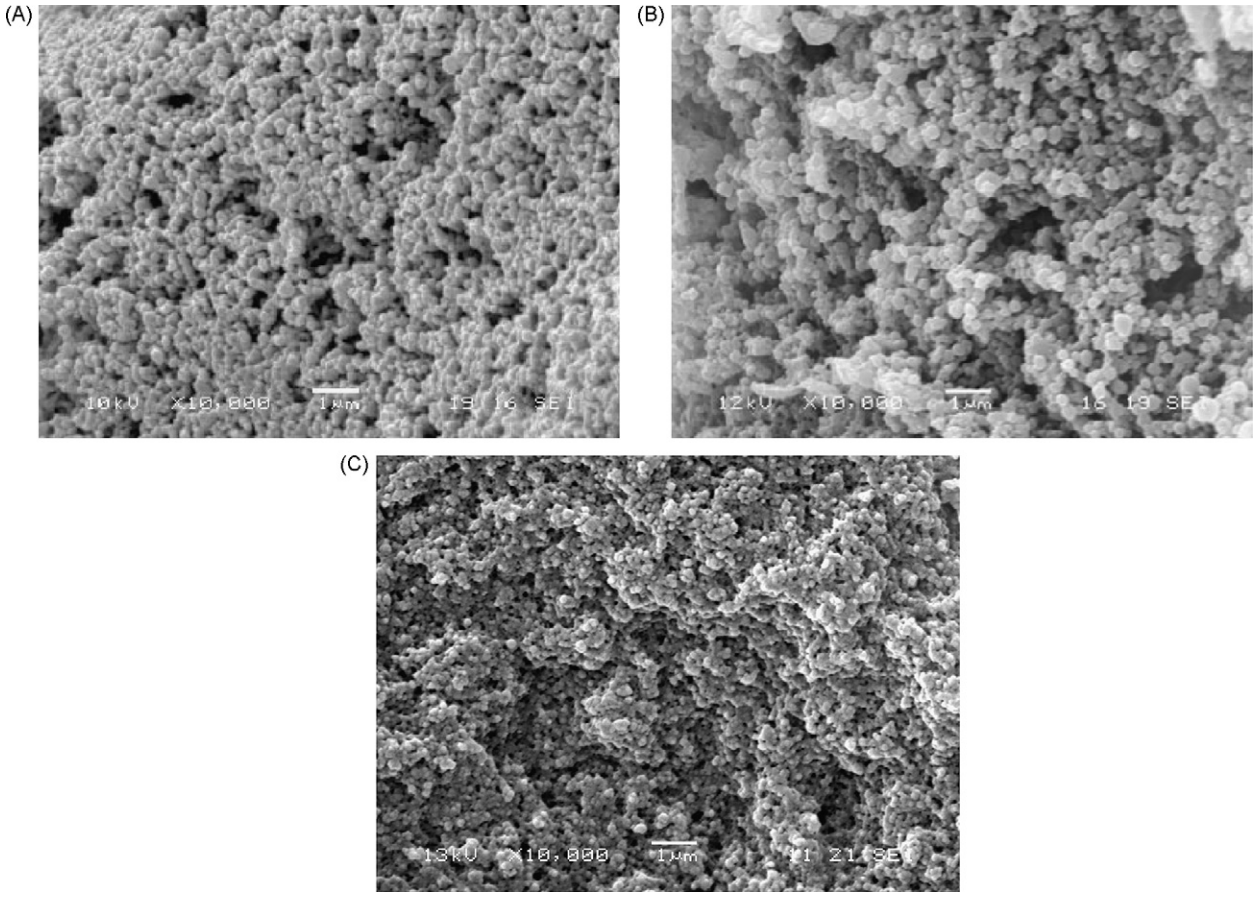

Fig. 2. SEM micrographs. (A) VAG nanoparticles sample, prepared with VAM41-S3 polymer. (B) 10TVAG-S7 nanoparticle formulation. (C) 10UPEG-Fab nanoparticle formulation.

was considered as reference value. All nanoparticles samples present a negative surface charge that was generated by the carboxyl ions belonging to the chain of all the considered polymers. Generally, the presence of Fab–SH moieties on the surface of targeted nanoparticles slightly reduced the zeta potential value. Conversely, the use of pegylated polymer matrices increased the zeta potential values of the nanoparticles. The effect is a consequence of the shielding activity of PEG chains, which shift the shear plane of the diffuse layer to a larger distance from nanoparticle surface thus decreasing the absolute value of the measured zeta potential (Gref et al., 1995). The use of covalently pegylated polymer matrices was extremely effective in the obtainment of a core–corona structure where the PEG moieties are extended out from the nanoparticle core into the aqueous environment (Avgoustakis, 2004; Hrkach et al., 1997). In these terms, it is possible to adjust PEG brushes length and density on particle surface by changing the composition of the starting material, giving better accuracy in respect to other strategies that lead to partial covalently bonded PEG moieties or physically adsorption of PEG chain on particle surface (Yoncheva et al., 2005, 2007). Concerning the complete biofunctionalized surface, including stealth-Fab grafted nanoparticles, the zeta potential value (−10.6 mV) fell within the range of values that in literature are considered to be the most effective to elude the

Table 4
Size distributions and *Z* potential values of stealth and targeted nanoparticles

Sample	Grafted molecule	Diameter (nm ± S.D.)[b]		*Z* pot (mV ± S.D.)
		Suspension[c]	Suspension[d]	
VAG-S7[a]	–	78 ± 52	14500 ± 9890	−18.5 ± 1.1
VAG–Fab	Fab–SH	88 ± 56	827 ± 916	−20.1 ± 1.1
VAG–PEG	PEG	130 ± 16	645 ± 884	−7.8 ± 0.5
VAG–PEG–Fab	PEG, Fab–SH	120 ± 15	740 ± 660	−10.6 ± 1.2

[a] Used as reference material.
[b] Diameter distribution by vol.%.
[c] Nanoparticle suspension before purification.
[d] Purified nanoparticles re-dispersed in physiological solution.

response of the reticuloendothelial system (RES) once the particles have entered the bloodstream (Gref et al., 1995, 2000; Müeller and Kissel, 1993; Li et al., 2001; Avgoustakis et al., 2003). Moreover, the presence of PEG on nanoparticles surface had a positive effect also on nanoparticles re-dispersion after centrifugation. PEG moieties determined a better recovery of nanoparticle diameter distributions in suspension and the formation of aggregates with a maximum mean diameter of 2 μm is minimum as indicated by pharmacopoeia requirements (Table 4).

3.2. Enzyme-loaded nanoparticles

Trypsin-loaded nanoparticles were prepared according to the VAG formulation by using trypsin dispersed in HSA in a proportion of 1 to 9 part by weight, which allowed for high trypsin loading without formation of macroscopic aggregates. Dimensional analysis and SEM characterization displayed monomodal size distribution with average diameter in the range of 130–150 nm (Fig. 2B).

Trypsin loading and activity maintenance were investigated by means of SEC and BApNA colorimetric assay, respectively. Preliminary SEC investigations on nanoparticle components alone and in mixtures evidenced that all nanoparticle components displayed well-resolved peaks with different retention times, except for low molecular weight VAM41-S7 that partially overlapped HSA peak. The analyses on mixtures of VAM41, HSA and porcine trypsin showed that there was an interaction between VAM41 polymers and HSA. The interaction was recorded by UV-vis and RI chromatograms displaying only one peak instead of two distinctly resolved peaks, as expected. This behavior is probably related to the known affinity of HSA for organic anions (Teresi and Murray Luck, 1952). The interaction of un-charged groups of the protein with non-polar portion of the polymer, in addition to the electrostatic attraction between protein and anion, is thought to be involved in the formation of VAM41–HSA complexes. Differently, trypsin did not interact with VAM41 and the peak assigned to the enzyme could always be identified. Once established that native trypsin and trypsin released by nanoparticles had the same retention time, the content of encapsulated enzyme was evaluated based on standard solutions of native trypsin. For nanoparticles prepared from low molecular weight polymers (VAM41-S6 and VAM41-S7), it was necessary to apply a peak deconvolution algorithm on nanoparticle chromatograms in order to distinguish the peaks belonging to the polymer–HSA complex and to the enzyme, respectively. In this case, the evaluation of trypsin loading resulted less accurate because of the implicit error committed in the processing of the data (Fig. 3A). The SEC analyses were compared to the trypsin activity evaluations. The results evidenced that when trypsin underwent the particle preparation process and relevant purification stage, the activity was maintained up to 42% of the original theoretical value and mostly it was recovered within the purified particles. Trypsin loading resulted very high especially with the low molecular weight VAM41-S7 polymer in 10TVAG-S7 formulation (78 ± 3%, w/w).

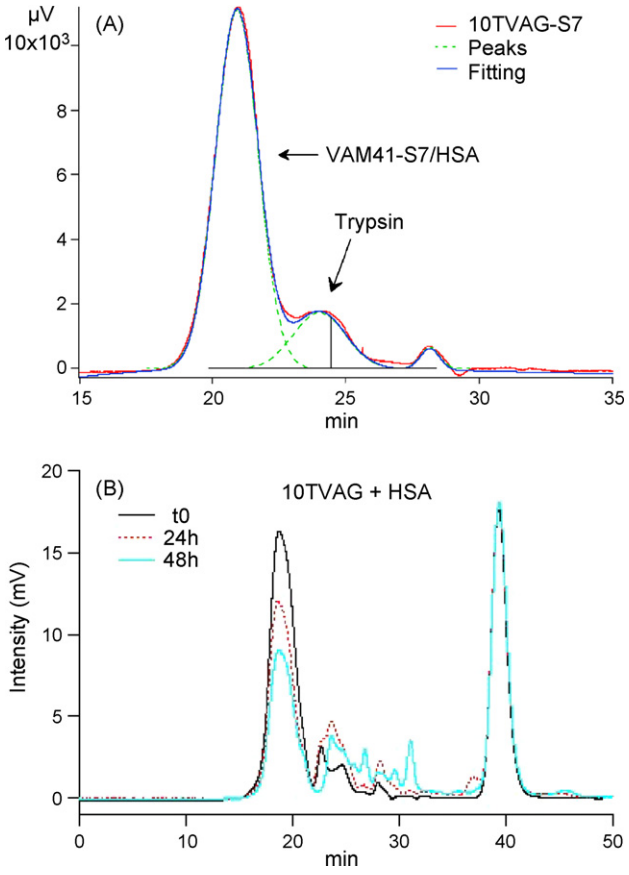

Fig. 3. SEC chromatograms. (A) Peak deconvolution analysis of SEC chromatogram recorded on sample 10TVAG-S7, UV detection at 280 nm. (B) SEC chromatograms of purified and dissolved 10TVAG particles after 0, 24 and 48 h of incubation with HSA (UV detection at 280 nm).

It is necessary to consider that, when trypsin is released from nanoparticles, the steric hindrance of polymer and stabilizer may reduce the access of natural macromolecular substrates to the enzyme active pocket and limit its proteolytic action on proteins. To assess trypsin activity maintenance toward medium sized proteins, the enzyme released from nanoparticles was tested against human serum albumin. The experiment was followed through SEC measurements based on previous observations reported by Lee and Park (1998). As shown in Fig. 3B, proteolytic activity of trypsin is preserved when the enzyme is released from the nanoparticles and the nanoparticle components do not interfere with trypsin activity toward medium sized proteins such as HSA. The reduction of VAM41–HSA peak (retention time 16–22 min) and the formation of low molecular weight fragments having longer retention times progressively proceeded in time and gave evidence of proteolytic activity of the released enzyme against albumin. When HSA substrate was not added to trypsin-loaded nanoparticles, the enzyme was still active toward the HSA employed in the preparation of the spheres. In this case, the production of low molecular weight fragments was less evident probably due to the low availability of HSA and to its strong interaction with the polymer. The peak at 37–42 min corresponded to acetyltryptophan, a stabilizer in HSA commercial product, here used as internal reference for SEC analyses.

Table 5
Activity of urokinase loaded into nanoparticles

Run	Polymer	Diameter[a] (nm ± S.D.)	EA[b] (UI/mg)
10UVAG-S6	VAM41-S6	132 ± 16	1780 ± 29
10UVAG-S7	VAM41-S7	149 ± 15	1500 ± 26
10UPEG	VAM41–PEG	124 ± 16	1800 ± 113
10UPEG–Fab	VAM41–PEG–Fab	128 ± 17	2500 ± 53

[a] Diameter distribution of nanoparticles by volume%.
[b] Encapsulated activity as urokinase amidolytic activity per mg of purified and dried nanoparticle.

The model enzyme trypsin was then replaced with urokinase, the thrombolytic agent. The use of urokinase did not affect nanoparticles size distribution and morphology. Nanoparticles were first prepared starting from low molecular weight polymers VAM41-S6 and VAM41-S7 and then by using the PEG and anti-fibrin Fab fragment-grafted polymers for the preparation of the final targeted-stealth nanoparticle delivery system (Fig. 2C).

Preliminary SEC analyses were performed on purified and dissolved urokinase-loaded nanoparticles. Urokinase is eluted separately from VAM41-S6/HSA peak (16–22 min), and the lack of peaks overlapping would allow in principle for the accurate evaluation of urokinase loading in nanoparticles, as based on the comparison to urokinase standard concentrations. Since maintenance of urokinase activity is extremely high, more than 80% as discussed below, it was decided to evaluate urokinase loading on the basis of its fibrinolytic activity instead of proceeding with SEC analyses.

The assessment of urokinase activity in both purified nanoparticle pellets and supernatants revealed that nanoparticles preparation and purification processes did not reduce significantly the activity of the enzyme. It was calculated that during the preparation of urokinase-loaded nanoparticles, the activity maintenance corresponded to 83% of original enzyme activity. Although urokinase and trypsin are highly homologous, the maintenance of their amidolytic activity resulted different. It is known that trypsin can show different molecular forms, that may affect the enzymatic activity, as consequence of a temperature- and pH-dependent stability. (Lazdunski and Delaage, 1967; Simon et al., 2001). Conversely, it is known that urokinase activity is stable between pH 4 and 10 when incubated at 37 °C (Celander and Guest, 1969; Kjeldgaard and Ploug, 1957). The higher activity maintenance in nanoparticles formation and purification may be thus related to a better stability of urokinase under the adopted analysis conditions. The activity of loaded urokinase was correlated to the dry weight of nanoparticles, to relatively compare the encapsulation efficiency obtained with different polymer matrices. A high encapsulated activity (EA) level was detected with both naked and biofunctionalized particles (Table 5). When stealth/urokinase-loaded nanoparticles were prepared, an improvement of EA was observed, combined with a drastic reduction in purification efficiency. This reduction was probably related to a lower conversion of the raw materials into nanoparticles during the preparation process, due to the better solubility in water of the pegylated polymers. The complete-targeted release system was obtained when the biofunctionalized and pegylated polymer matrix was applied for the preparation of urokinase-loaded nanoparticles. The anti-fibrin targeted, stealth, urokinase-loaded nanoparticles displayed a monomodal diameter distribution, with a mean diameter of 128 nm and EA higher than that recorded in all the other formulated particles. Purification efficacy was compatible with the results obtained with the analogous stealth particles. The activity of encapsulated urokinase was about 40% higher than the activity of stealth and naked nanoparticles. Additional investigations will be carried out to get a better insight into the obtained results. In a forthcoming paper, the preparation of urokinase-loaded targeted nanoparticles, based on VAM41–Fab polymer, will be considered and the role of Fab fragments in improving urokinase encapsulation will be reported.

3.2.1. *In vitro* drug release studies

Release kinetics studies were performed on urokinase-loaded nanoparticles; HSA-loaded nanoparticles and urokinase alone were used as blank and reference, respectively.

Fig. 4A shows the release profile of HSA from nanoparticles and the diffusion of the protein through the dialysis membrane, used as control. It is evident that the diffusion step was faster than the release process and it did not affect the release kinetics profile. As expected by a controlled drug release system, the release of the proteins from nanoparticles was time con-

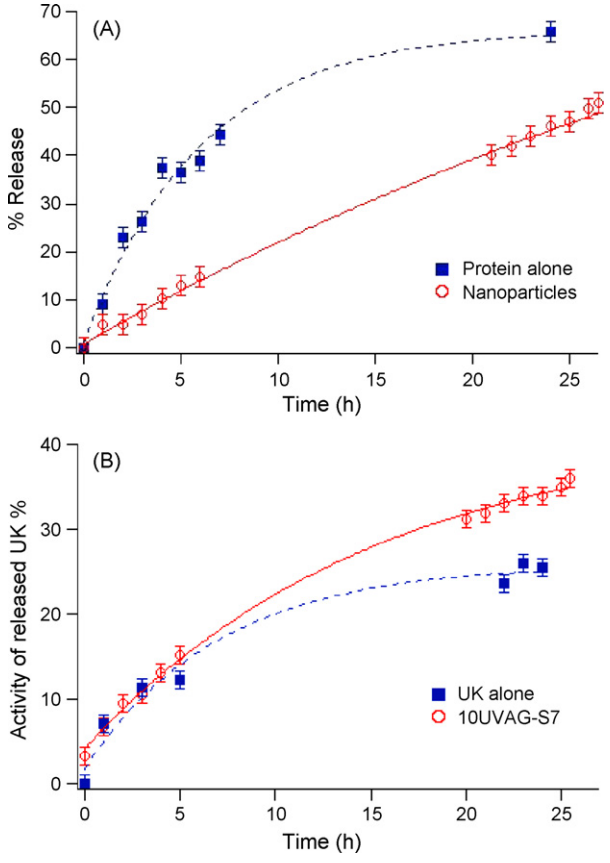

Fig. 4. *In vitro* drug release studies. (A) Profile of HSA release from nanoparticles and diffusion of the protein through the dialysis membrane. (B) Activity of urokinase as control sample and as released from nanoparticles.

trolled and did not display an initial burst step. The enzymatic activity of the urokinase released from nanoparticles was also evaluated. As described above, the experiment was performed at 37 °C in PBS 0.05 M pH 7.4. In these conditions, urokinase is stable at least for 30 min (Ploug and Ole, 1957) but with longer time is subjected to autolysis and consequently to lose some activity towards the substrate. The loss in activity could be monitored on plain urokinase control sample by comparing the results from BCA and S-2444 assays performed on the enzyme diffused outside of the dialysis membrane. BCA and S-2444 assays provided information on urokinase concentration outside the membrane and its activity, respectively. It was first observed that although plain urokinase diffusion through the membrane was fast, the enzyme easily lost its activity evidencing no correspondence between urokinase concentration in solution and expected activity. Conversely, when urokinase-loaded nanoparticles were placed inside the membrane and compared to plain urokinase solutions, it was noticed that the enzyme released from nanoparticles preserves its activity longer than the control samples (Fig. 4B). In particular, during the first 4 h, the activity displayed by the enzyme released from nanoparticles was equal with the activity of the fresh urokinase control sample; at longer time the control sample showed lower activity levels than the urokinase released from nanoparticles.

The results gave evidence that the release of enzyme from nanoparticles is time controlled and that nanoparticles have a preserving effect on urokinase activity in solution. Therefore, it was assessed that in case of administration of urokinase-loaded nanoparticles targeted to fibrin clot by covalent conjugation with anti-fibrin Fab fragments, the enzyme would preserve its thrombolytic properties in a more efficient way with respect to free drug administration. The encapsulation method adopted in the present work for the preparation of urokinase-loaded nanoparticles resulted less aggressive than other strategies and did not significantly altered the activity of the two tested enzymes (trypsin and urokinase) because it avoided the direct modification of the active proteins (Naik et al., 2005).

3.3. Stability studies

The directive 2001/83/EC of the European Parliament and of the Council of 6 November 2001 on the Community code relating to medicinal products for human use reports specific guidelines for stability tests, being an essential investigation to define appropriate storage conditions, determine the shelf life, verify the formation of by-products, and significant alteration of the product upon storage. Stability programs of urokinase-loaded bioerodible nanoparticles were setup on urokinase shelf life, that is 2 years at 5–3 °C as indicated by the manufacturer (Abbokinase, Alfakinasi). Storage, shipment, and subsequent use of the final product were considered for the preparation of a typical final pharmaceutical dosage form, for the selection of the storage conditions and time duration of the stability studies.

As a typical final pharmaceutical dosage form either lyophilized nanoparticles or injectable nanoparticle suspension were evaluated. Both dosage forms were required to be sterile and sterile filtration through 0.22 μm membrane filters in aseptic environment was considered as the most appropriate method since it has no adverse effect on either polymer or drug (Konan et al., 2002). The developed drug delivery system resulted suitable for sterile filtration, particle diameter distribution was preserved and no significant membrane clogging was observed.

Freeze-drying is commonly applied to pharmaceutics to obtain dry powder that are easy to handle, allow for better long term storage and improve physical and chemical stability of the material. This method is particularly indicated for thermally labile biological compounds, but requires the use of stabilizing agents and additives to avoid the formation of sticky soft powders that are very difficult to be re-dispersed in injectable media (Allison et al., 1999; Ward et al., 1999; Anchordoquy et al., 2001; Bozdag et al., 2005). Mannitol was selected as cryo/lyo-protecting agent, because it is generally recommended for parenteral route administration and it had previously been applied in polymeric nanoparticles lyophilization studies (Konan et al., 2002; Bozdag et al., 2005; Chacón et al., 1999; Saez et al., 2000). Mannitol acted as an efficient lyoprotector agent and the re-dispersion of lyophilized nanospheres was appreciably improved in the presence of 7% by weight of this compound. It was also observed that the lyophilization of urokinase-loaded nanoparticles in 7% mannitol did not significantly alter the activity of the encapsulated enzyme, with the preservation of 70% of its starting loaded activity.

3.3.1. Stability of lyophilized nanoparticles

The stability of the employed polymeric materials was previously assessed under stressed conditions, 35 ± 0.5 °C for 13 weeks, and accelerated conditions, 25 ± 2 °C for 6 months (Chiellini et al., in press). In the present work, similar stability conditions were first applied to VAG nanoparticles and subsequently the attention was focused on enzyme-loaded nanoparticles. The stability of VAG nanoparticles was assessed from a morphological point of view by means of SEM micrographs. Although this type of analysis is commonly affected by statistical factors and accordingly not very reproducible, the results indicated that naked nanoparticles were not affected by major morphological changes under both stressful and accelerated storage conditions.

Lyophilized sterile urokinase-loaded nanoparticles underwent stressed stability studies. Nanoparticles stability was assessed by investigating nanoparticles morphology and activity maintenance of the encapsulated enzyme. As displayed in Fig. 5A, no significant alteration in urokinase activity was noticed for both nanoparticles and plain urokinase, used as control. Diameter distribution of the re-dispersed samples was also preserved (Fig. 5B). The obtained results are in agreement with what observed on lyophilized recombinant streptokinase (freezing temperature: −50 °C) kept at 37 °C for 6 months, as reported in literature (López et al., 2004). Furthermore, the stability studies performed on urokinase-loaded nanoparticles confirmed that the occurrence of unexpected events such as short failure of the cold chain during storage or transportation of a putative final product would not induce significant alteration in polymer and

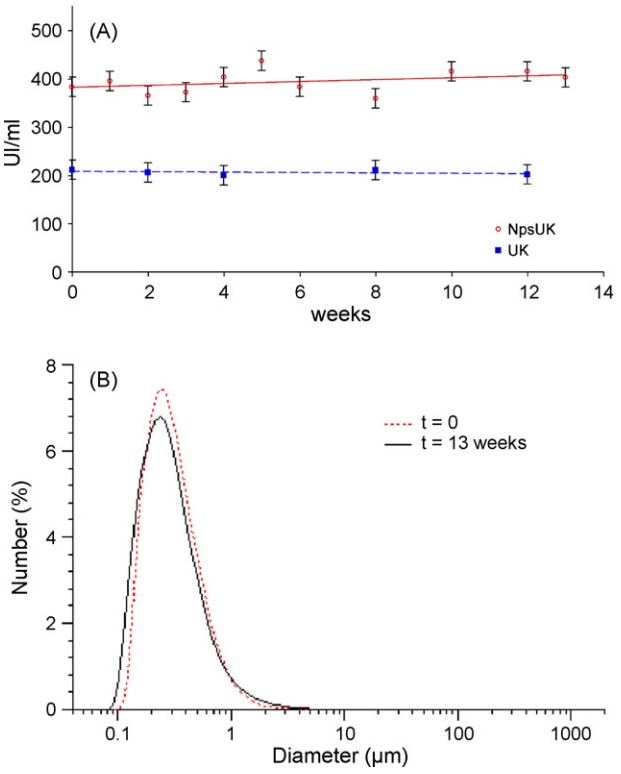

Fig. 5. Stability investigations. (A) Trends of the activity maintenance in urokinase-loaded nanoparticles (NPsUK) and control (urokinase alone, UK) as recorded under stressed conditions. (B) Diameter distribution of urokinase-loaded nanoparticles re-dispersed in water, before and at the end of the stressed stability program.

stabilizer properties, particle morphology, enzyme activity and suspension granulometry.

3.3.2. Stability studies of bioerodible nanoparticles in suspension

Stability tests of nanoparticles in suspensions were performed in order to investigate alternative storage conditions. Sterile suspensions of naked nanoparticles were kept in the dark at 4 °C and at room temperature (21 ± 3 °C) for 15 months and dimensional analyses were carried out at various time points. In all cases, the same identical monomodal distribution with 126 ± 16 nm mean diameter was recorded and after 15 months the aspect of the suspensions was milky and homogeneous without any detectable sediment, similarly to the freshly prepared suspension.

Analogous conditions were applied for the evaluation of the stability of urokinase-loaded nanoparticles in suspensions 10UVAG-S7. In agreement with what observed for naked nanoparticles suspensions, no relevant variations in diameter distribution (from 89 ± 87 to 81 ± 53 nm) and in enzyme activity (from 4881 ± 359 to 5223 ± 85 UI/ml), were registered after 18 months; thus indicating a high stability of the nanoparticles in suspension. It is interesting to notice that in the present work, the investigated storage conditions, nanoparticles in suspension maintain their morphology, size distribution, and do not show any leakage of the encapsulated enzyme, that completely preserves its amidolytic activity.

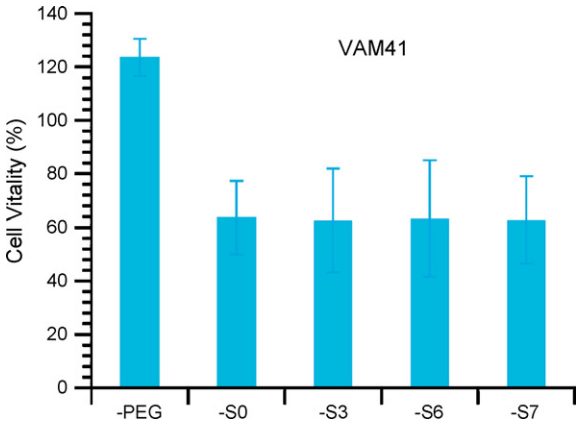

Fig. 6. WST-1 assay, cytotoxicity evaluation of bioerodible nanoparticles. Data represent mean values ± S.D. of three independent experiments carried out in triplicates.

3.4. Cytotoxicity evaluation

In order to be considered suitable for biomedical applications, new biopolymeric constructs must undergo a series of *in vitro* and *in vivo* tests to assess their biocompatibility. Concerning *in vitro* cytotoxicity tests, the high sensitivity of these assays is guaranteed by restricted cell culture conditions and by the absence of the protective mechanisms that support cells *in vivo* (ISO 10993). They are rapid, not expensive and represent the first step in the evaluation of biocompatibility.

The biocompatibility of VAM41-Sx and of the relevant matrices grafted with PEG and Fab had already been assessed both *in vitro* and *in vivo* (Chiellini et al., in press). In the present study, bioerodible nanoparticles based on VAM41-Sx polymer series were purified and tested *in vitro*, on Mouse embryo fibroblasts balb 3T3 clone A31, for the evaluation of cytotoxicity by means of WST-1 assay. The results showed that, in general, the toxicity of the prepared systems is fairly low with cell viability higher than 60% in respect of control cell. Moreover the evaluation of long-circulating nanoparticles (prepared with pegylated polymer matrices) indicated the full cytocompatibility of the prepared samples with 100% cell viability in respect to the control. This observation confirms that the exposure of PEG moieties on nanoparticles surface is reflected in a considerable increase of nanoparticles biocompatibility (Fig. 6).

4. Conclusions

In the present work, different aspects of the development of new pharmaceutical nanocolloids for the controlled release of drugs have been investigated. The research started from the selection of a conventional therapy regime suitable to be replaced by a controlled drug delivery system, based on nanostructured final dosage forms. The design and synthesis of polymeric matrices satisfactorily enabling the achievement of the proposed target were realized (Chiellini et al., in press). The optimization of nanostructured dosage forms was undertaken and followed by the characterization of the releasing profiles and activity maintenance of the loaded enzymes (trypsin and urokinase) as well

as by the assessment of their biocompatibility *in vitro* and the processing into conventional freeze-dried or colloidal dosage forms. Indeed, the developed systems can be considered a suitable model of controlled drug delivery nanoconstructs, in the form of soft bioerodible nanoparticles, provided of targeting and stealth features and that in principle could be adapted to address other therapeutic regimes involving conventional and macromolecular drugs administration.

Acknowledgements

The results reported in the present paper have been generated within the framework of the EC-funded project TATLYS G5RD-CT-2000-0291. The authors wish to acknowledge the financial support by EC and the contribution given by Mr. Piero Narducci in recording SEM images of nanoparticles.

References

Allison, S.D., Chang, B., Randolph, T.W., Carpenter, J.F., 1999. Hydrogen bonding between sugar and protein is responsible for inhibition of dehydration-induced protein unfolding. Arch. Biochem. Biophys. 365, 289–298.

Anchordoquy, T.J., Izutsu, K.I., Randolph, T.W., Carpenter, J.F., 2001. Maintenance of quaternary structure in the frozen state stabilizes lactate dehydrogenase during freeze-drying. Arch. Biochem. Biophys. 390, 35–41.

Avgoustakis, K., Beletsi, A., Panagi, Z., Klepetsanis, P., Livaniou, E., Evangelatos, G., Ithakissios, D.S., 2003. Effect of copolymer composition on the physicochemical characteristics, in vitro stability, and biodistribution of PLGA–mPEG nanoparticles. Int. J. Pharm. 259, 115–127.

Avgoustakis, K., 2004. Pegylated poly(lactide) and poly(lactide-*co*-glycolide) nanoparticles: preparation, properties and possible application in drug delivery. Curr. Drug Delivery 1, 321–333.

Barlow, G.H., Lazer, L., 1972. Characterization of the plasminogen activator isolated from human embryo kidney cells: comparison with urokinase. Thromb. Res. 1, 201–208.

Bell, W.R., 2002. Thrombolytic solutions, therapeutic agents. pharmacokinetics and pharmacodynamics. Rev. Cardiovasc. Med. 3, S34–S44.

Bergstrom, R.C., Coombs, G.S., Ye, S., Madison, E.L., Goldsmith, E.J., Corey, D.R., 2003. Binding of nonphysiological protein and peptide substrates to proteases: differences between urokinase-type plasminogen activator and trypsin and contributions to the evolution of regulated proteolysis. Biochemistry 42, 5395–5402.

Bernik, M.B., Whiate, W.F., Oiler, E.P., Kwaan, H.C., 1974. Immunologic identity of plasminogen activator in human urine, heart, blood vessels and tissue culture. J. Lab. Clin. Med. 84, 546–558.

Bozdag, S., Dillen, K., Vandervoort, J., Ludwig, A., 2005. The effect of freeze-drying with different cryoprotectants and gamma-irradiation sterilization on the characteristics of ciprofloxacin HCl-loaded poly(D,L-lactide-glycolide) nanoparticles. J. Pharm. Pharmacol. 57, 699–708.

Breschi, M.C., Chiellini, E., Morganti, F., Solaro, R., 1996. New structurally modified cyclodextrins for controlled release of antihypertensive drugs. In: Ogata, N., Kim, S.W., Feijen, J., Okano, T. (Eds.), Advanced Biomaterials in Biomedical Engineering and Drug Delivery Systems. Springer-Verlag, Tokyo, p. 335.

Celander, D.R., Guest, M.M., 1969. The biochemistry and physiology of urokinase. Am. J. Cardiol. 6, 409–419.

Chacón, M., Molpeceres, J., Berges, L., Guzman, M., Aberturas, M.R., 1999. Stability and freeze-drying of cyclosporine loaded poly(D,L lactide-glycolide) carriers. Eur. J. Pharm. Sci. 8, 99–107.

Chiellini, E., Solaro, R., D'Antone, S., Bemporad, L., 1991 Polyfunctional derivatives of cyclodextrin. Eur. Pat. 91830497.3.

Chiellini, E., Solaro, R., Leonardi, G., Giannasi, D., Lisciani, R., Mazzanti, G., 1992. New polymeric hydrogel formulations for the controlled release of α-interferon. J. Control. Release 22, 273–282.

Chiellini, F., Piras, A.M., Gazzarri, M., Bartoli, C., Ferri, M., Paolini, L., Chiellini, E., 2008. Bioactive polymeric materials for targeted administration of active agents—synthesis and evaluation. Macromol. Biosci., doi:10.1002/mabi.200700228.

Cowdall, J., Davies, J., Roberts, M., Carlsson, A., Solaro, R., Mazzanti, G., Chiellini, E.E., Chiellini, F., Soderlind, E., 1999a. Microparticles based on hybrid polymeric materials for controlled release of biologically active molecules. A process for preparing the same and their uses for in vivo and in vitro therapy, prophylaxis and diagnostics. PCT Int. Appl. N. WO9902131.

Cowdall, J., Davies, J., Roberts, M., Carlsson, A., Solaro, R., Mazzanti, G., Chiellini, E.E., Chiellini, F., Soderlind, E., 1999b. Microparticles for controlled delivery of biologically active molecules. PCT Int. Appl. N. WO9902135.

Craig, C.R., Stitzel, R.E., 1994. Farmacologia Moderna Con Applicazioni Cliniche. Antonio Delfino Editore, Roma, Italy.

Gref, R., Domb, A., Quellec, P., Blunk, T., Muller, R.H., Verbavatz, J.M., Langer, R., 1995. The controlled intravenous delivery of drugs using PEG-coated sterically stabilized nanospheres. Adv. Drug Delivery Rev. 16, 215–233.

Gref, R., Luck, M., Quellec, P., Marchand, M., Dellacherie, E., Harnisch, S., Blunk, T., Muller, R.H., 2000. Stealth corona–core nanoparticles surface modified by polyethylene glycol (PEG): influences of the corona (PEG chain length and surface density) and of the core composition on phagocytic uptake and plasma protein adsorption. Colloids Surf. B: Biointerf. 18, 301–313.

Hoste, K., Schacht, E., Seymour, L., 2000. New derivatives of polyglutamic acid as drug carrier systems. J. Control. Release 64, 53–61.

Hrkach, J.S., Peracchia, M.T., Domb, A., Lotans, N., Langer, R., 1997. Nanotechnology for biomaterials engineering: structural characterization of amphiphilic polymeric nanoparticles by 1H NMR spectroscopy. Biomaterials 18, 27–30.

Katzung, B.G., 2000. Farmacologia Generale E Clinica IV Italian Edition Based on VII English Edition. PICCIN nuova libraria, SpA, Padova, Italy.

Kjeldgaard, N.O., Ploug, J., 1957. Urokinase an activator of plasminogen from human urine. II. Mechanism of plasminogen activation. Biochim. Biophys. Acta 24, 283–289.

Konan, Y.N., Gurny, R., Allemann, E., 2002. Preparation and characterization of sterile and freeze-dried sub-200 nm nanoparticles. Int. J. Pharm. 233, 239–252.

Kubik, T., Bogunia-Kubik, K., Sugisaka, M., 2005. Nanotechnology on duty in medical applications. Curr. Pharm. Biotechnol. 6, 17–33.

Lazdunski, M., Delaage, M., 1967. Étude structurale du trypsinogéne et de la trypsine, Les diagrammes d' état. Biochim. Biophys. Acta 140, 417–434.

Lee, H., Park, T.G., 1998. Conjugation of trypsin by temperature-sensitive polymers containing a carbohydrate moiety: thermal modulation of enzyme activity. Biotechnol. Prog. 14, 508–516.

Li, Y.P., Pei, Y.Y., Zhang, X.Y., Gu, Z.H., Zhou, Z.H., Yuan, W.F., Zhou, J.J., Zhu, J.H., Gao, X.J., 2001. PEGylated PLGA nanoparticles as protein carriers: synthesis, preparation and biodistribution in rats. J. Control. Release 1, 203–211.

lkjaersig, N., Fletcher, A.P., Sherry, S., 1958. The activation of human plasminogen. II. A kinetic study of activation with trypsin, urokinase, and streptokinase. J. Biol. Chem. 233, 86–90.

López, M., González, L.R., Reyes, N., Sotolongo, J., Pujol, V., Aroche, K., 2004. Stabilization of a freeze-dried recombinant streptokinase formulation without serum albumin. J. Clin. Pharm. Ther. 29, 367–373.

Müeller, B.G., Kissel, T., 1993. Camouflage nanospheres: a new approach to bypassing phagocytic blood clearance by surface modified particulate carriers. Pharm. Pharmacol. Lett. 3, 67–70.

Naik, S.S., Liang, J.F., Park, Y.J., Lee, W.K., Yang, V.C., 2005. Application of "ATTEMPTS" for drug delivery. J. Control. Release 101, 35–45.

Park, T.G., Lu, W., Crotts, G., 1995. Importance of in vitro experimental conditions on protein release kinetics, stability and polymer degradation in protein encapsulated poly(D,L-lactic acid-*co*-glycolic acid) microspheres. J. Control. Release 33, 211–222.

Pawar, R., Ben-Ari, A., Domb, A.J., 2004. Protein and peptide parental controlled delivery. Expert. Opin. Biol. Ther. 4, 1203–1212.

Ploug, J., Ole, K.N., 1957. Urokinase an activator of plasminogen from human urine. I. Isolation and properties. Biochim. Biophys. Acta 24, 278–282.

Saez, A., Guzman, M., Molpeceres, J., Aberturas, M.R., 2000. Freeze-drying of polycaprolactone and poly(D,L-lactic-glycolic) nanoparticles induce minor particle size changes affecting the oral pharmacokinetics of loaded drugs. Eur. J. Pharm. Biopharm. 50, 379–387.

Simon, M.L., László, K., Kotormán, M., Szajáni, B., 2001. A comparative study of the conformational stabilities of trypsin and chymotrypsin. Acta Biol. 45, 43–49.

Teresi, J.D., Murray Luck, J., 1952. The combination of organic anions with serum albumin. J. Biol. Chem. 194, 823–834.

Ward, K.R., Adams, G.D.J., Alpar, H.O., Irwin, W.J., 1999. Protection of the enzyme L-asparaginase during lyophilisation—a molecular modelling approach to predict required level of lyoprotectant. Int. J. Pharm. 187, 153–162.

Yoncheva, K., Lizarraga, E., Irache, J.M., 2005. Pegylated nanoparticles based on poly(methyl vinyl ether-*co*-maleic anhydride): preparation and evaluation of their bioadhesive properties. EUFEPS 24, 411–419.

Yoncheva, K., Guembe, L., Campanero, M.A., Irache, J.M., 2007. Evaluation of bioadhesive potential and intestinal transport of pegylated poly(anhydride) nanoparticles. Int. J. Pharm. 334, 156–165.

Zambaux, M.F., Bonneaux, F., Gref, R., Dellacherie, E., Vigneron, C., 1999. Preparation and characterization of protein C-loaded PLA nanoparticles. J. Control. Release 60, 179–188.